

ON-LINE APPENDIX 1

Seoul Neuropsychological Screening Battery

The Korean version of the Mini-Mental State Examination was used to screen for general cognitive status. The Seoul Neuropsychological Screening Battery, which was used to determine cognitive status, comprises a forward and backward digit span; letter-cancellation tests; reading, writing, comprehension, repetition; confrontational naming by using the Korean version of the Boston Naming Test¹; finger naming; right/left orientation; body part identification; calculation; ideomotor; buccofacial praxis; drawing interlocking pentagons; 3-word registration, recall, and recognition; the Seoul Verbal Learning Test; the Rey Complex Figure Test, including immediate recall, 20-minute delayed recall, recognition; motor impersistence; contrasting program; the Go-No-Go test; fist-edge-palm; alternating hand movements; alternating square and triangle; Luria loop; the phonemic and semantic Controlled Oral Word Association Test; and the Stroop test, covering attention, language, visuospatial function, verbal and visual memory, and frontal executive function.

Age-, sex-, and education-specific norms for each test were available on the basis of 447 healthy subjects. When the scores of these tests were below the 16th percentiles of the norms for age-, sex-, and education-matched healthy subjects, outcomes were classified as abnormal. With the exception of the language domain, 2 neuropsychological tests were designated to represent each of the 4 cognitive domains: 1) Attention (forward and backward digit span and Stroop Color and Word Test); 2) Executive function (phonemic and semantic Controlled Oral Word Association Test and Clock Drawing Test); 3) Memory (Seoul Verbal Learning Test and Rey Complex Figure Test); 4) Visuospatial Function (Rey Complex Figure Test copy and pentagon drawing test); and 5) Language Domain (Korean version of the Boston Naming Test). According to the diagnostic criteria recommended by the Movement Disorder Society Task Force,² PD-MCI was diagnosed when there were impairments on at least 2 tests from the 4 domains (attention, executive function, memory, and visuospatial function domains) (level 2) or when there were impairment in the language domain and at least 1 test from the other 4 domains (level 1).

ON-LINE APPENDIX 2

Cortical Thickness Analysis

At first, the native MR imaging data of all subjects were registered into the International Consortium for Brain Mapping 152 symmetric template by using a linear transformation and were corrected for intensity nonuniformity artifacts.³⁻⁵ A hierarchic multiscale nonlinear fitting algorithm was then applied to normalize the individual MR images in stereotaxic space and to provide a priori information (ie, tissue probability maps for subsequent tissue classification by using the neural network classifier).^{3,6} An artificial neural network classifier was applied to identify GM, WM, and CSF. Partial volume errors, involving MR imaging intensity-mixing at the tissue interfaces due to the finite resolution of the imaging device, were estimated and corrected by using a trimmed minimum covariance determinant method.^{6,7} Estimating the fractional amount of each tissue type within each voxel improved the accuracy of cortical surface extraction.⁷ Hemi-

spheric cortical surfaces were automatically extracted from each MR imaging volume by using the constrained Laplacian-based automated segmentation with proximities algorithm, which reconstructed the inner cortical surface by deforming a spheric mesh onto the WM/GM boundary and then expanded the deformable model to the GM/CSF boundary.^{8,9}

Previous studies have shown that human cortices are not simply scaled versions of one another, and the expansion of WM rather than GM would be favored in larger brains.^{10,11} Because cortical surface mesh models for each hemisphere were initially extracted from MR imaging volumes previously transformed into stereotaxic space, the inverse transformation was then applied to the cortical surfaces so that cortical thickness could be measured in native space. The inner and outer cortical surfaces had the same number of vertices (40,962), and cortical thickness was measured by calculating the Euclidean distance between linked vertices on the WM/GM boundary surface and the GM/CSF intersection surface.^{9,12,13} To ensure an optimal correspondence at each vertex of the cortical surface model across individuals, we used an iterative surface registration algorithm with an unbiased iterative group template showing enhanced anatomic detail.¹⁴ Diffusion smoothing, which generalized the Gaussian kernel smoothing with a 20-mm full width at half maximum kernel, was used to increase the signal-to-noise ratio and optimally detect population changes. This kernel size was chosen to maximize the statistical power while minimizing false-positives.¹³ The localized regional differences of cortical thickness among groups were analyzed by applying an ANCOVA with age, sex, years of education, age at onset of parkinsonism, and levodopa-equivalent dose entered as covariates. A false discovery rate threshold of $P < .05$ was used to control for multiple comparisons.¹⁵

ON-LINE APPENDIX 3

Tract-Based Spatial Statistics Analysis

Motion artifacts and eddy current distortions were first corrected by normalization of each directional volume to the non-diffusion-weighted volume (B0) by using the FMRIB Linear Image Registration Tool (FLIRT; <http://www.fmrib.ox.ac.uk/>) with 6 *df*. Then, the diffusion tensor was calculated by using a simple least-squares fit of the tensor model, and fractional anisotropy, mean diffusivity, axial diffusivity, and radial diffusivity maps were computed for each voxel by using standard methods for the DTIFit program in FSL (http://fsl.fmrib.ox.ac.uk/fsl/fsl-4.1.9/fdt/fdt_dtifit.html). All fractional anisotropy images were aligned to the standard FMRIB58_FA template (http://fsl.fmrib.ox.ac.uk/fsl/fslwiki/FMRIB58_FA), which was provided by the FSL program by using a nonlinear registration algorithm implemented in the Tract-Based Spatial Statistics package.

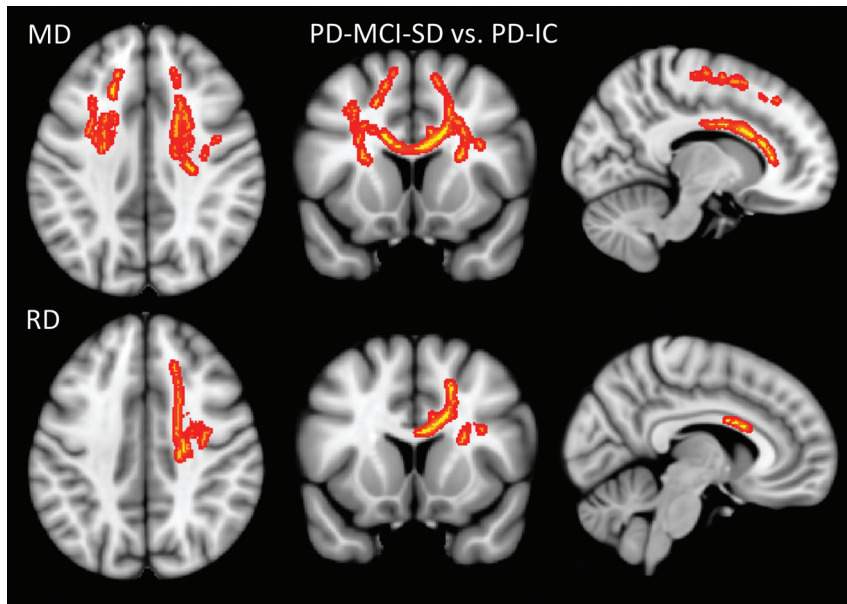
The fractional anisotropy images were then averaged to create a mean fractional anisotropy skeleton. Each subject's aligned fractional anisotropy images were projected onto this skeleton by filling each voxel on the skeleton with the maximum fractional anisotropy values from a plane perpendicular to the local skeleton structure.¹⁶ To exclude voxels of adjacent GM or CSF, we chose a threshold fractional anisotropy value of 0.2. The mean diffusivity, axial diffusivity, and radial diffusivity maps were also processed by using the same methods used in the fractional anisotropy maps by

applying the nonlinear registration algorithm and projecting them onto the mean fractional anisotropy skeleton.

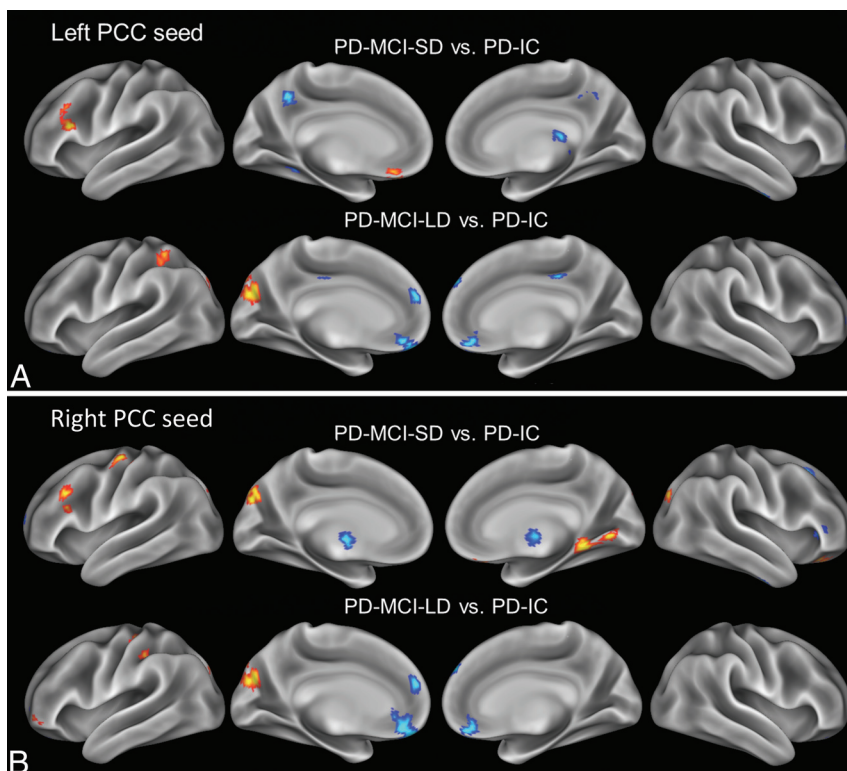
Voxelwise statistical analysis of individual skeleton images was performed by using a nonparametric permutation-based 2-sample t test to compare the DTI values for each group pair. In the ANCOVA, age, sex, years of education, age at onset of parkinsonism, and levodopa-equivalent dose were included as covariates. The null distribution was built up over 5000 permutations. The threshold-free cluster enhancement approach with the 2D parameter settings was used for control over the multiple comparison correction.¹⁷ The results for each DTI value were considered significant at a family-wise error-corrected $P < .05$. To identify WM tracts, we used 2 WM atlases within FSL (<http://fsl.fmrib.ox.ac.uk/fsl/data/atlas-descriptions.html>), the Johns Hopkins University WM tractography atlas and the International Consortium for Brain Mapping-DTI-81 WM labels atlas.

REFERENCES

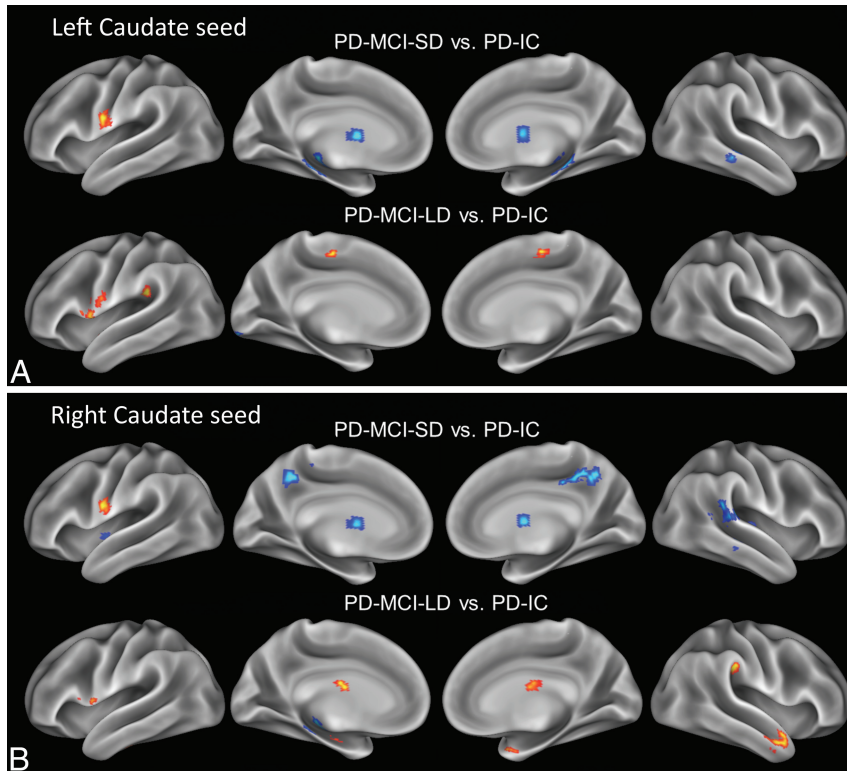
1. Kim H, Na DL. **Normative data on the Korean version of the Boston Naming Test.** *J Clin Exp Neuropsychol* 1999;21:127–33 CrossRef Medline
2. Litvan I, Goldman JG, Tröster AI, et al. **Diagnostic criteria for mild cognitive impairment in Parkinson's disease: Movement Disorder Society Task Force guidelines.** *Mov Disord* 2012;27:349–56 CrossRef Medline
3. Collins DL, Neelin P, Peters TM, et al. **Automatic 3D intersubject registration of MR volumetric data in standardized Talairach space.** *J Comput Assist Tomogr* 1994;18:192–205 Medline
4. Sled JG, Zijdenbos AP, Evans AC. **A nonparametric method for automatic correction of intensity nonuniformity in MRI data.** *IEEE Trans Med Imaging* 1998;17:87–97 Medline
5. Grabner G, Janke AL, Budge MM, et al. **Symmetric atlas and model based segmentation: an application to the hippocampus in older adults.** *Med Image Comput Comput Assist Interv* 2006;9(pt 2): 58–66 Medline
6. Zijdenbos AP, Forghani R, Evans AC. **Automatic "pipeline" analysis of 3-D MR imaging data for clinical trials: application to multiple sclerosis.** *IEEE Trans Med Imaging* 2002;21:1280–91 Medline
7. Tohka J, Zijdenbos A, Evans A. **Fast and robust parameter estimation for statistical partial volume models in brain MRI.** *Neuroimage* 2004;23:84–97 Medline
8. Kim JS, Singh V, Lee JK, et al. **Automated 3-D extraction and evaluation of the inner and outer cortical surfaces by using a Laplacian map and partial volume effect classification.** *Neuroimage* 2005;27: 210–21 Medline
9. MacDonald D, Kabani N, Avis D, et al. **Automated 3-D extraction of inner and outer surfaces of cerebral cortex from MRI.** *Neuroimage* 2000;12:340–56 Medline
10. Im K, Lee JM, Lyttelton O, et al. **Brain size and cortical structure in the adult human brain.** *Cereb Cortex* 2008;18:2181–91 Medline
11. Lüders E, Steinmetz H, Jäncke L. **Brain size and gray matter volume in the healthy human brain.** *Neuroreport* 2002;13:2371–74 Medline
12. Kabani N, Le Goualher G, MacDonald D, et al. **Measurement of cortical thickness by using an automated 3-D algorithm: a validation study.** *Neuroimage* 2001;13:375–80 Medline
13. Lerch JP, Evans AC. **Cortical thickness analysis examined through power analysis and a population simulation.** *Neuroimage* 2005;24: 163–73 Medline
14. Lyttelton O, Boucher M, Robbins S, et al. **An unbiased iterative group registration template for cortical surface analysis.** *Neuroimage* 2007;34:1535–44 Medline
15. Genovese CR, Lazar NA, Nichols T. **Thresholding of statistical maps in functional neuroimaging by using the false discovery rate.** *Neuroimage* 2002;15:870–78 Medline
16. Smith SM, Jenkinson M, Johansen-Berg H, et al. **Tract-based spatial statistics: voxelwise analysis of multi-subject diffusion data.** *Neuroimage* 2006;31:1487–505 Medline
17. Smith SM, Nichols TE. **Threshold-free cluster enhancement: addressing problems of smoothing, threshold dependence and localization in cluster inference.** *Neuroimage* 2009;44:83–98 CrossRef Medline



ON-LINE FIG 1. Tract-Based Spatial Statistics analysis in PD-MCI-SD and PD-IC groups. Warm colors indicate increased DTI values in the PD-MCI-SD group compared with the PD-IC group ($P < .05$, family-wise error-corrected). Images are oriented according to neurological convention (right is right).



ON-LINE FIG 2. RSFC analysis in PD-MCI and PD-IC groups by using the PCC as a seed. Warm colors indicate increased connectivity, and cool colors indicate decreased connectivity in each PD-MCI group compared with the PD-IC group. All demonstrated clusters are significant at the $P < .05$ level with correction for multiple comparisons.



ON-LINE FIG 3. RSFC analysis in the PD-MCI and PD-IC groups by using the caudate as the seed. Warm colors indicate increased connectivity, and cool colors indicate decreased connectivity in each PD-MCI group compared with the PD-IC group. All demonstrated clusters are significant at the $P < .05$ level, with correction for multiple comparisons.

On-line Table 1: Neuropsychological data in de novo PD-IC group and PD-MCI groups according to the duration of parkinsonism prior to MCI^a

Cognitive Subdomains	De Novo PD-IC (n = 15)	PD-MCI-SD (n = 16)	PD-MCI-LD (n = 43)	P Value ^b	Post Hoc Analysis		
					P1 ^c	P2 ^d	P3 ^e
Attention							
Digit Span (forward)	7 (6–9)	6 (5–9)	6 (4–9)	.454	–	–	–
Digit Span (backward)	4 (3–7)	3.5 (3–5)	4.0 (2–6)	.091	–	–	–
Digit Span total	11.1 ± 1.7	10.1 ± 1.6	10.1 ± 2.3	.216	–	–	–
Word Stroop test	112 (112–112)	112 (96–112)	112 (90–112)	.068	–	–	–
Color Stroop test	94.8 ± 19.6	68.7 ± 21.2	80.1 ± 20.0	.003	.002	.052	.174
Executive function							
Phonemic generative naming	27 (13–44)	14 (8–31)	18 (4–44)	<.001	<.001	.003	.243
COWAT (Animal)	16.3 ± 4.6	13.6 ± 2.8	13.2 ± 3.9	.031	.157	.028	1.000
COWAT (Supermarket)	18.8 ± 4.7	13.1 ± 3.9	15.0 ± 4.7	.003	.002	.021	.452
Clock Drawing Test	10 (10–10)	10 (2–10)	9 (4–10)	.006	.063	.003	.945
Verbal memory function							
SVLT							
Free recall	20.7 ± 3.5	17.6 ± 3.4	17.1 ± 5.1	.029	.172	.025	1.000
Delayed recall	7.5 ± 1.6	4.3 ± 2.4	4.3 ± 2.5	<.001	.001	<.001	1.000
Recognition	21.5 ± 1.2	20.1 ± 2.6	20.2 ± 1.9	.067	–	–	–
Visual memory function (RCFT)							
Immediate recall	19.5 ± 6.0	12.0 ± 6.0	11.6 ± 5.5	<.001	.002	<.001	1.000
Delayed recall	18.1 ± 4.8	11.5 ± 6.3	11.9 ± 5.4	.001	.004	.001	1.000
Recognition	20.9 ± 1.3	19.5 ± 1.5	19.7 ± 2.0	.060	–	–	–
Visuospatial function							
RCFT copy	35.0 (32.0–36.0)	31.5 (18.0–36.0)	33.0 (17.5–36.0)	.013	.006	.012	1.000
Pentagon drawing test	1 (1–1)	0 (0–1)	1 (0–1)	.408	–	–	–
Language and related function							
K-BNT	48.5 ± 4.7	42.1 ± 7.5	42.1 ± 8.6	.023	.077	.024	1.000
Other indices							
Contrasting program	20 (18–20)	20 (18–20)	20 (7–20)	.785	–	–	–
Go-No-Go test	20 (18–20)	20 (10–20)	20 (1–20)	.682	–	–	–
Semantic generative naming	32 (26–59)	27 (18–37)	28 (14–46)	.011	.009	.042	1.000

Note:—COWAT indicates the Controlled Oral Word Association Test; SVLT, Seoul Verbal Learning Test; K-BNT, the Korean version of the Boston Naming Test; –, not significant; RCFT, Rey Complex Figure Test.

^a Values that have normal distribution are expressed as means; otherwise, values are expressed as median (range).

^b P values for comparison among 3 groups.

^c P values for comparison between de novo PD-IC and PD-MCI-SD groups.

^d P values for comparison between de novo PD-IC and PD-MCI-LD groups.

^e P values for comparison between PD-MCI-SD and PD-MCI-LD groups.

On-line Table 2: Regions showing significant differences in functional connectivity when PCC was used as a seed

Seed	Region	Side	MNI Coordinates			Maximum <i>T</i>	No. of Voxels	<i>P</i> Value
			x	y	z			
PCC_L								
PD-IC > PD-MCI-SD	Inferior temporal gyrus	R	45	-9	42	4.51	16	<.001
	Middle frontal gyrus	R	30	66	9	4.48	24	<.001
	Thalamus	R	18	-30	6	4.16	14	<.001
	Precuneus	L	-12	-54	45	4.15	38	<.001
	Parahippocampal gyrus	L	-33	-57	-3	3.37	16	.001
	Cerebellum	L	-6	-63	-48	3.44	21	.001
PD-IC < PD-MCI-SD	Rectus gyrus	L	-6	36	-21	4.28	19	<.001
	Inferior frontal gyrus	L	-45	21	27	4.04	26	<.001
PD-IC > PD-MCI-LD	Superior frontal gyrus	R	9	57	39	3.93	18	<.001
	Medial frontal gyrus	L	-6	51	24	3.89	12	<.001
	Superior frontal gyrus	R	24	45	6	3.85	15	<.001
	Middle cingulate	R/L	0	-27	45	3.58	16	<.001
PD-IC < PD-MCI-LD	Medial frontal gyrus	L	-6	57	-24	3.49	89	.001
	Superior occipital gyrus	L	-12	-78	27	4.8	85	<.001
	Inferior parietal lobule	L	-30	-84	42	3.65	39	<.001
	Middle occipital gyrus	L	-27	-63	30	3.22	12	.001
PD-MCI-SD < PD-MCI-LD	Inferior parietal lobule	L	-36	-48	54	3.15	13	.001
	Hippocampus	L	-24	-36	-3	3.8	21	<.001
	Postcentral gyrus	L	-30	-39	45	3.3	21	<.001
PD-MCI-SD > PD-MCI-LD	Thalamus	R/L	0	-24	12	3.28	18	.001
	Middle cingulate	L	-3	-24	48	4.75	22	<.001
	Insula	R	33	27	-21	4.05	12	<.001
	Medial frontal gyrus	L	6	54	27	4.03	101	<.001
	Medial frontal gyrus	L	-6	54	24	3.88	71	<.001
	Inferior temporal gyrus	R	33	6	-42	3.88	20	<.001
	Precentral gyrus	R	39	-18	66	3.73	21	<.001
	Superior frontal gyrus	L	-12	27	51	3.5	47	<.001
	Inferior frontal gyrus	L	-51	30	9	3.32	20	.001
	PCC_R							
PD-IC > PD-MCI-SD	Inferior temporal gyrus	R	45	-9	-39	5.38	19	<.001
	Superior frontal gyrus	R	18	21	48	3.84	15	<.001
	Superior frontal gyrus	L	-27	63	12	3.57	13	.001
PD-IC < PD-MCI-SD	Lingual gyrus	R	9	-69	3	4.9	50	<.001
	Precentral gyrus	L	-42	-21	60	4.57	26	<.001
	Inferior frontal gyrus	L	-45	21	33	4.12	24	<.001
	Cuneus	L	-6	-81	39	4.09	57	<.001
	Orbitofrontal gyrus	R	18	39	-15	3.96	30	<.001
	Superior occipital gyrus	R	33	-84	30	3.7	24	.001
PD-IC > PD-MCI-LD	Medial frontal gyrus	L	-6	51	24	4.64	24	<.001
	Medial frontal gyrus	L	-3	45	-12	4.5	151	<.001
	Superior frontal gyrus	R	9	57	39	3.76	16	<.001
PD-IC < PD-MCI-LD	Cuneus	L	-9	-81	27	5.04	67	<.001
	Superior occipital gyrus	L	-21	-87	39	3.69	19	<.001
	Middle frontal gyrus	L	-45	54	-3	3.67	21	<.001
	Postcentral gyrus	L	-33	-27	45	3.45	31	.001
	Middle occipital gyrus	L	-30	-69	33	3.32	22	.001
PD-MCI-SD < PD-MCI-LD	Inferior parietal lobule	L	-30	-39	42	4.33	21	<.001
	Thalamus	L	-21	-18	3	3.84	13	<.001
	Cuneus	L	-9	-105	-12	3.29	16	.001
PD-MCI-SD > PD-MCI-LD	Cuneus	R	18	-63	15	3.21	13	.001
	Inferior frontal gyrus	R	39	-18	18	3.98	12	<.001
	Precentral gyrus	R	36	-18	66	3.59	13	<.001
	Inferior temporal gyrus	R	36	3	-42	3.55	12	<.001
	Medial frontal gyrus	L	-6	51	24	3.53	22	<.001
Orbitofrontal gyrus	L	-27	27	-15	3.34	12	.001	

Note:—L indicates left; R, right; MNI, Montreal Neurological Institute.

On-line Table 3: Regions showing significant differences in functional connectivity when the caudate was used as a seed

Seed	Region	Side	MNI Coordinates			Maximum T	No. of Voxels	P Value		
			x	y	z					
Caudate_L	PD-IC > PD-MCI-SD	Middle temporal gyrus	R	60	-30	-6	4.31	24	<.001	
		Caudate	L	-3	-3	9	4.03	27	<.001	
		Parahippocampal gyrus	R	18	-27	-12	3.95	14	<.001	
	PD-IC < PD-MCI-SD	Parahippocampal gyrus	L	-15	-33	-6	3.91	12	<.001	
		Pre/postcentral gyrus	L	-51	-6	18	5.13	36	<.001	
		Middle frontal gyrus	R	33	51	33	4.13	14	<.001	
	PD-IC > PD-MCI-LD	Orbitofrontal gyrus	R	21	60	-9	3.07	12	.003	
		Fusiform gyrus	L	-18	-84	-18	3.77	25	<.001	
		Parahippocampal gyrus	R	15	6	-27	4.14	13	<.001	
	PD-IC < PD-MCI-LD	Postcentral gyrus	L	-54	0	18	3.9	12	<.001	
		Supramarginal gyrus	L	-48	-33	27	3.61	13	<.001	
		Cerebellum	L	-3	-48	-39	3.6	13	<.001	
	PD-MCI-SD < PD-MCI-LD	Precentral gyrus	L	-60	9	3	3.46	13	.001	
		Supplementary motor area	R	6	-18	54	3.29	13	.001	
		Globus pallidus	R	21	3	3	4.04	22	<.001	
		Middle frontal gyrus	L	-36	33	33	3.81	40	<.001	
		Middle cingulate	R	12	-6	48	3.53	15	<.001	
		Superior frontal gyrus	R	18	51	24	3.45	12	.001	
		Superior temporal gyrus	L	-54	3	-3	3.45	13	.001	
		Caudate	L	-3	-3	12	3.32	16	.001	
		Middle frontal gyrus	L	-18	24	54	3.16	15	.001	
		Middle cingulate	L	-3	21	36	3.09	16	.002	
		PD-MCI-LD < PD-MCI-SD	Superior parietal lobule	L	-21	-57	60	3.73	18	<.001
			Inferior parietal lobule	L	-27	-75	36	3.52	20	<.001
	Middle occipital gyrus		R	42	-78	9	3.4	14	.001	
	Caudate_R	PD-IC > PD-MCI-SD	Putamen	R	24	6	6	5.49	12	<.001
			Putamen	R	30	-21	6	5.02	23	<.001
			Middle cingulate	R	15	3	33	4.62	12	<.001
			Caudate	L	0	-3	9	4.62	15	<.001
			Precuneus	L	-9	-51	45	4.58	20	<.001
			Superior temporal gyrus	R	63	-45	18	4.36	14	<.001
			Insula	L	-48	-6	3	4.31	20	<.001
			Middle temporal gyrus	R	60	-30	-6	4.02	12	<.001
Precuneus			R	6	-51	42	3.97	51	<.001	
Superior temporal gyrus			R	63	-36	12	3.87	26	<.001	
PD-IC < PD-MCI-SD			Postcentral gyrus	L	-51	-9	18	4.25	23	<.001
			Thalamus	L	-18	-21	-6	4.24	15	<.001
		Middle temporal gyrus	R	54	6	-24	4.17	33	<.001	
PD-IC > PD-MCI-LD		Parahippocampal gyrus	R	18	6	-27	3.99	19	<.001	
		Inferior frontal gyrus	L	-60	9	6	3.86	13	<.001	
		Supramarginal gyrus	R	57	-33	36	3.86	19	<.001	
		Hippocampus	L	-45	-18	-18	3.69	13	<.001	
		Middle frontal gyrus	R	36	48	30	3.61	13	<.001	
		Thalamus	R	3	-12	18	3.52	15	<.001	
		PD-MCI-SD < PD-MCI-LD	Superior temporal gyrus	L	-51	-15	3	4.56	43	<.001
			Middle frontal gyrus	L	-36	33	33	4.38	13	<.001
			Inferior temporal gyrus	R	51	-27	-21	3.93	13	<.001
			Middle temporal gyrus	L	-60	-24	6	3.86	27	<.001
			Middle frontal gyrus	L	-42	45	15	3.85	16	<.001
			Insula	R	45	-9	12	3.82	16	<.001
Caudate			L	-3	-3	12	3.7	20	<.001	
Putamen			L	-27	6	-3	3.5	17	<.001	
Middle temporal gyrus			R	54	-51	12	3.38	17	.001	
PD-MCI-LD < PD-MCI-SD			Globus pallidus	R	21	-12	-3	4.11	15	<.001
			Angular gyrus	L	-48	-48	30	3.99	31	<.001
			Angular gyrus	R	42	-60	57	3.91	33	<.001
		Parahippocampal gyrus	R	24	-36	-3	3.68	15	<.001	
		Cerebellum	R	27	-69	-30	3.64	35	<.001	
	Middle temporal gyrus	R	48	-69	6	3.43	14	.001		
	Inferior parietal lobule	L	-36	-66	57	3.22	14	.001		

Note:—L indicates left; R, right; MNI, Montreal Neurological Institute.